Chem Biol Drug Des 2016; **87:** 283–289

Research Article

Design, Synthesis, and Biological Evaluation of Novel 2-(Pyridin-3-yloxy)acetamide Derivatives as Potential Anti-HIV-1 Agents

Boshi Huang[1], Xiao Li[1], Peng Zhan[1,*], Erik De Clercq[2], Dirk Daelemans[2], Christophe Pannecouque[2] and Xinyong Liu[1,*]

[1]Department of Medicinal Chemistry, Key Laboratory of Chemical Biology (Ministry of Education), School of Pharmaceutical Sciences, Shandong University, 44 West Culture Road, Ji'nan 250012, Shandong, China
[2]Rega Institute for Medical Research, KU Leuven Minderbroedersstraat 10, Leuven B-3000, Belgium
**Corresponding authors: Peng Zhan and Xinyong Liu, zhanpeng1982@sdu.edu.cn and xinyongl@sdu.edu.cn*

Through a structure-based molecular hybridization and bioisosterism approach, a series of novel 2-(pyridin-3-yloxy)acetamide derivatives were designed, synthesized, and evaluated for their anti-HIV activities in MT-4 cell cultures. Biological results showed that three compounds (Ia, Ih, and Ij) exhibited moderate inhibitory activities against wild-type (wt) HIV-1 strain (III_B) with EC_{50} values ranging from 8.18 μM to 41.52 μM. Among them, Ij was the most active analogue possessing an EC_{50} value of 8.18 μM. To further confirm the binding target, four compounds were selected to implement an HIV-1 RT inhibitory assay. In addition, preliminary structure–activity relationship (SAR) analysis and some predicted physicochemical properties of three active compounds Ia, Ih, and Ij were discussed in detail. Molecular docking studies were also carried out to investigate the binding modes of Ij and the lead compound GW678248 in the binding pocket of RT, which provided beneficial information for further rational design of non-nucleoside reverse transcriptase inhibitors.

Key words: anti-HIV activity, bioisosterism, HIV-1 RT, molecular hybridization, non-nucleoside reverse transcriptase inhibitors

Received 16 June 2015, revised 15 August 2015 and accepted for publication 27 August 2015

Due to the unique antiviral potency, high specificity and low cytotoxicity, HIV-1 non-nucleoside reverse transcriptase inhibitors (NNRTIs) have become indispensable components of highly active antiretroviral therapy (HAART), an efficient and standard treatment regimen for AIDS therapy (1). Up to date, five NNRTI drugs (Figure S1), including the first generation NNRTIs (nevirapine, delavirdine, efavirenz) and the second generation NNRTIs (etravirine, rilpivirine), have been approved by FDA for clinical use, and significantly reduced the morbidity and mortality of AIDS. However, long-term use of NNRTIs inevitably leads to the rapid emergence of viral drug resistance and serious adverse effects (2). Therefore, the development of novel NNRTI drugs with efficient anti-HIV-1 potency against both wild-type (wt) and mutant strains is still urgently required to combat the increasing AIDS pandemic (3).

Fortunately, the structural diversity of HIV-1 NNRTIs and the flexibility of NNRTI binding pocket (NNIBP) in RT gave a broad space for novel lead discovery, and the pharmacophore similarity of NNRTIs also provided valuable clues to expedite process of lead discovery and optimization (4).

Benzophenone derivatives are one representative class of HIV-1 NNRTIs with excellent activities against wt and a wide range of drug-resistant HIV-1 strains. Among them, GW678248 (**1**) (Figure S2) displayed remarkable inhibitory activities against wt, K103N single mutant and K103N + Y181C double mutant strains in the nanomolar range, with EC_{50} values of 0.52, 1.0, and 1.4 nM accordingly, and its prodrug is undergoing phase II clinical trials (5,6).

Arylthiotetrazolyl acetanilide analogue **2**, which was discovered in the course of a ultra high-throughput screening (uHTS) campaign, exhibited strong inhibition against wt and the clinically relevant K103N + Y181C double mutant HIV-1 RT, in low nanomolar and submicromolar level, respectively. Subsequent structural modifications led to the identification of compound **3**, which possesses some different chemical features, such as parazole scaffold instead of tetrazole scaffold and oxygene instead of sulfur. Surprisingly, compound **3** showed a dramatically increased inhibitory activity against K103N + Y181C double mutant RT (7) (Figure S2).

In continuation of developing potent NNRTIs as promising antiretroviral agents, a series of 2-(pyridin-3-yloxy)acetamide derivatives were designed derived from the privileged structures of lead compounds GW678248 (**1**) and **3**

 doi: 10.1111/cbdd.12657

utilizing the molecular hybridization and bioisosterism principles. In the newly designed compounds, a naphthyl or a *para*-substituted phenyl was adapted from compound **3**, which was reported to occupy the aromatic-rich subpocket in NNIBP. And a pyridyl ring, as a common surrogate of phenyl ring, was used as the central ring based on bioisosterism. Furthermore, the right oxyacetamide moiety was employed from the two lead compounds with the aim of generating indispensable interactions with RT at the RT/solvent interface. Different substituents, varying in electronic nature and size, were applied in the right phenyl wing for further investigating the structure–activity relationship (SAR) features of the newly synthesized compounds (Figure S3).

Herein, we reported the synthesis and antiviral activity in vitro of these novel 2-(pyridin-3-yloxy)acetamide derivatives. The SARs were well discussed, and the molecular modeling study and the molecular physicochemical property analysis were also carried out to gain further insights into this series of analogues.

Experimental Section

Chemistry

All melting points (mp) were determined on a micromelting point apparatus and are uncorrected. Mass spectra were performed on a LC Autosampler Device: Standard G1313A instrument by electrospray ionization. ^{1}H NMR and ^{13}C NMR spectra were obtained on a Bruker AV-400 spectrometer (Bruker BioSpin, Fällanden, Switzerland) in the indicated solvent DMSO-d_6. Chemical shifts were expressed in δ units (p.p.m.), using TMS as an internal standard, and J values were reported in hertz (Hz). TLC was performed on Silica Gel GF254. Spots were visualized by irradiation with UV light (λ 254 nm). Flash column chromatography was carried out on columns packed with silica gel 60 (200–300 mesh). Solvents were of reagent grade and, if needed, were purified and dried by standard methods. The key reagents were purchased from commercial suppliers and with no further purification when used. Rotary evaporators were served in concentration of the reaction solutions under reduced pressure.

General procedure for the synthesis of intermediates (I–V)

2-(Naphthalen-1-yl)pyridin-3-ol (**I**): The starting material 2-bromopyridin-3-ol (**S**) (0.20 g, 1.14 mmol), 1-naphthylboric acid (0.24 g, 1.38 mmol), K_2CO_3 (0.24 g, 1.72 mmol), and $Pd(PPh_3)_4$ (0.09 g, 0.08 mmol) were added to a mixed solvent (dioxane: water = 5 mL: 1 mL). The mixture was stirred at 90 °C under a nitrogen atmosphere until the completion of the reaction as detected by TLC. After cooling to room temperature, the solid was filtered, washed by water, and the total filtrate was extracted with EtOAc (3 × 40 mL). The combined organic phase was washed with saturated brine and dried over anhydrous Na_2SO_4, filtered and concentrated under reduced pressure. Recrystallization of the residue by methanol afforded intermediate **I** as a white solid, which could be used in the next step with no further purification. Yield: 55%. mp: 177.0–177.8 °C. ^{1}H NMR (400 MHz, DMSO-d_6, p.p.m.) δ: 9.84 (s, 1H, OH), 8.20 (d, J = 4.44 Hz, 1H, pyridine-H), 7.96 (t, J = 6.84 Hz, 2H, Naph-H), 7.59–7.38 (m, 6H, Naph-H, pyridine-H), 7.32 (dd, J = 8.16 Hz, J = 4.52 Hz, 1H, pyridine-H), ^{13}C NMR (100 MHz, DMSO-d_6, p.p.m.) δ: 152.19, 146.82, 140.47, 136.77, 133.60, 131.65, 128.51, 128.33, 127.79, 126.36, 126.24, 126.07, 125.72, 124.17, 123.26. ESI-MS: *m/z* 220.4 (M-1), $C_{15}H_{11}NO$ (221.08).

2-(*p*-Tolyl)pyridin-3-ol (**II**): A mixture of 2-bromopyridin-3-ol (**S**) (0.20 g, 1.14 mmol), *p*-tolylboronic acid (0.19 g, 1.38 mmol), K_3PO_4 (0.61 g, 2.30 mmol), and $Pd(PPh_3)_4$ (0.09 g, 0.08 mmol) was dissolved in a mixed solvent (dioxane: water = 5 mL: 1 mL). The solution was stirred at 90 °C under a nitrogen atmosphere followed by TLC until its completion. After evaporation of the excess solvent under reduced pressure, water was added and the solution was extracted with CH_2Cl_2 (3 × 40 mL). The organic layer was combined, washed with saturated brine, dried over anhydrous Na_2SO_4, filtered and concentrated under reduced pressure. Finally, the residue was further purified by flash column chromatography and subsequently recrystallized with methanol to give pure intermediate **II** as a white solid. Yield: 36%. mp: 193.0–194.0 °C. ^{1}H NMR (400 MHz, DMSO-d_6, p.p.m.) δ: 10.08 (s, 1H, OH), 8.14 (d, J = 4.40 Hz, 1H, pyridine-H), 7.93 (d, J = 8.12 Hz, 2H, Ph-H), 7.31 (d, J = 8.12 Hz, 1H, pyridine-H), 7.23 (d, J = 8.04 Hz, 2H, Ph-H), 7.16 (dd, J = 8.12 Hz, J = 4.48 Hz, 1H, pyridine-H), 2.34 (s, 3H, CH_3), ^{13}C NMR (100 MHz, DMSO-d_6, p.p.m.) δ: 151.86, 144.89, 140.57, 137.47, 135.70, 129.19 (2 × Ph-C), 128.78 (2 × Ph-C), 123.89, 123.46, 21.32 (CH_3). ESI-MS: *m/z* 184.2 (M-1), $C_{12}H_{11}NO$ (185.08).

III–**V** were prepared according to the same procedure described as **II**, while amount of the initial materials and reaction solvents extended 10 times accordingly.

2-(4-(Trifluoromethyl)phenyl)pyridin-3-ol (**III**): White solid, yield: 43%. mp: 234.6–235.4 °C. ^{1}H NMR (400 MHz, DMSO-d_6, p.p.m.) δ: 10.45 (s, 1H, OH), 8.26 (d, J = 8.16 Hz, 2H, Ph-H), 8.21 (d, J = 4.28 Hz, 1H, pyridine-H), 7.80 (d, J = 8.28 Hz, 2H, Ph-H), 7.40 (d, J = 8.12 Hz, 1H, pyridine-H), 7.28 (dd, J = 8.16 Hz, J = 4.40 Hz, 1H, pyridine-H), ^{13}C NMR (100 MHz, DMSO-d_6, p.p.m.) δ: 152.53, 142.92, 142.38, 140.99, 129.86, 128.40 (q, J_{C-F} = 32.00 Hz, 2C, Ph-C), 125.12 (q, J_{C-F} = 4.00 Hz, 2C, Ph-C), 124.88 (q, J_{C-F} = 270.00 Hz, 2C, Ph-C), 124.84, 124.48. ESI-MS: *m/z* 240.2 (M + 1), $C_{12}H_8F_3NO$ (239.06).

2-(4-(*tert*-Butyl)phenyl)pyridin-3-ol (**IV**): White solid, yield: 32%. mp: 176.0–176.6 °C. ^{1}H NMR (400 MHz, DMSO-d_6,

p.p.m.) δ: 10.07 (s, 1H, OH), 8.14 (d, J = 4.40 Hz, 1H, pyridine-H), 7.94 (d, J = 8.40 Hz, 2H, Ph-H), 7.44 (d, J = 8.44 Hz, 2H, Ph-H), 7.31 (d, J = 8.12 Hz, 1H, pyridine-H), 7.16 (dd, J = 8.08 Hz, J = 4.48 Hz, 1H, pyridine-H), 1.32 (s, 9H, *t*-Bu), ^{13}C NMR (100 MHz, DMSO-d_6, p.p.m.) δ: 151.89, 150.60, 144.97, 140.61, 135.70, 129.02 (2 × Ph-C), 124.92 (2 × Ph-C), 123.84, 123.47, 34.77, 31.60 (3 × CH_3). ESI-MS: *m/z* 228.6 (M + 1), $C_{15}H_{17}NO$ (227.13).

2-(4-Methoxyphenyl)pyridin-3-ol (**V**): Yellow solid, yield: 40%. mp: 180.0–180.6 °C. ^{1}H NMR (400 MHz, DMSO-d_6, p.p.m.) δ: 10.07 (s, 1H, OH), 8.12 (d, J = 4.28 Hz, 1H, pyridine-H), 8.02 (d, J = 8.76 Hz, 2H, Ph-H), 7.29 (d, J = 8.00 Hz, 1H, pyridine-H), 7.14 (dd, J = 8.08 Hz, J = 4.48 Hz, 1H, pyridine-H), 6.98 (d, J = 8.80 Hz, 2H, Ph-H), 3.80 (s, 3H, CH_3), ^{13}C NMR (100 MHz, DMSO-d_6, p.p.m.) δ: 159.44, 151.61, 144.60, 140.50, 130.96, 130.58 (2 × Ph-C), 123.81, 123.07, 113.60 (2 × Ph-C), 55.55 (OCH_3). ESI-MS: *m/z* 203.3 (M+2), $C_{12}H_{11}NO_2$ (201.08).

General procedure for the synthesis of target compounds (Ia-o, IIa, IIb, IIIa, IIIb, IVa, IVb, Va, Vb)

At room temperature, key intermediates **I–V** (0.15 g, 1 eqv.) and anhydrous K_2CO_3 (2 eqv.) were added to anhydrous *N,N*-Dimethylformamide (DMF, 5 mL), followed by the addition of the appropriate $ClCH_2CONHAr$ (1 eqv.). Then, the reaction mixture was stirred until its completion at 50 °C. The excess DMF was evaporated under reduced pressure, and H_2O (40 mL) was added. After extraction with EtOAc (3 × 40 mL), the combined organic phase was washed with saturated brine, dried over anhydrous Na_2SO_4, filtered and concentrated under reduced pressure. Then, the residue was further purified by flash column chromatography and recrystallized with EtOAc or anhydrous methanol to afford pure title compounds **Ia-o**, **IIa, IIb**, **IIIa**, **IIIb**, **IVa**, **IVb**, **Va** and **Vb**.

In vitro *anti-HIV assay*

Evaluation of the antiviral activity and cytotoxicity of the synthesized compounds was performed using the MTT assay as previously described (8,9). Stock solutions (10× final concentration) of test compounds were added in 25 μL volumes to two series of triplicate wells to allow simultaneous evaluation of their effects on mock- and HIV-infected cells at the beginning of each experiment. Serial fivefold dilutions of test compounds were made directly in flat-bottomed 96-well microtitre trays by adding 100 μL medium to the 25 μL stock solution and transferring 25-μL of this solution to another well that contained 100 μL medium using a Biomek 3000 robot (Beckman Instruments, Fullerton, CA, USA). Untreated control HIV- and mock-infected cell samples were included for each sample. HIV-1 wt strain (IIIB), HIV-1 double mutant strain (RES056) or HIV-2 strain (ROD) stock (50 μL) at 100–300 CCID50 (50% cell culture infectious dose) or culture medium was added to either the infected or mock-infected wells of the microtitre tray. Mock-infected cells were used to evaluate the effect of test compounds on uninfected cells to assess its cytotoxicity. Exponentially growing MT-4 cells were centrifuged for 5 min at 1000 rpm, and the supernatant was discarded. The MT-4 cells were resuspended at 6×10^5 cells/mL, and 50 μL volumes were transferred to the microtitre tray wells. Five days after infection, the viability of mock- and HIV-infected cells was examined spectrophotometrically by the MTT method. The 50% cytotoxic concentration (CC_{50}) was defined as the concentration of the test compound that reduced the viability of the mock-infected MT-4 cells by 50%. The concentration achieving 50% protection from the cytopathic effect of the virus in infected cells was defined as the 50% effective concentration (EC_{50}).

HIV-1 RT inhibition assay

The inhibition assay of HIV-1 RT_{wt} was performed by utilizing the template/primer hybrid poly(A) × oligo$(dT)_{15}$, digoxigenin- and biotin-labeled nucleotides, an antibody to digoxigenin which was conjugated to peroxidase (anti-DIG-POD), and the peroxidase substrate ABTS. The incorporation quantities of the digoxigenin- and biotin-labeled dUTP into DNA represented the activity of HIV-1 RT. The HIV-RT inhibition assay was implemented using an RT assay kit (Roche, Mannheim, Germany), and the procedures for assaying RT inhibition were carried out as described in the kit protocol (10). Concretely, the reaction mixture consisted of template/primer complex, 2′-deoxynucleotide-5′-triphosphates (dNTPs), and RT enzyme in the lysis buffer with or without inhibitors. After incubation for 1 h at 37 °C, the reaction mixture was transferred to streptavidine-coated microtitre plate (MTP). The biotin-labeled dNTPs that are incorporated in the template due to the presence of RT were bound to streptavidine. The unbound dNTPs were washed using wash buffer, and then, antidigoxigenin–peroxidase (anti-DIG-POD) was added in MTP. The DIG-labeled dNTPs incorporated in the template was bound to anti-DIG-POD antibody. The unbound anti-DIG-POD was also washed elaborately for five times using wash buffer, and finally, the peroxide substrate (ABST) was added to the MTP. A colored reaction product emerged during the cleavage of the substrate catalyzed by a peroxide enzyme. The absorbance of the sample was determined at OD_{450} using MTP ELISA reader. The percentage inhibitory activity of RT inhibitors was calculated by comparison with a sample lacking an inhibitor. The resulting color intensity is directly proportional to RT activity. The percentage inhibitory values were calculated by the following formula: %Inhibition = [O.D. value without inhibitors (with RT) -O.D. value with RT and inhibitors]/[O.D. value with RT and inhibitors-O.D. value without RT and inhibitors]. The IC_{50} value corresponded to the concentration of the tested compound required to inhibit the incorporation of the labeled dUTP into RT by 50%.

Molecular simulations

The molecules (**Ij** and the lead compound GW678248) for docking were optimized for 2000-generations until the maximum derivative of energy became 0.005 kcal/(mol*Å), using the Tripos force field. Charges were computed and added according to Gasteiger–Huckel parameters. The published 3D crystal structures of wt RT complexes (PDB code: 3DLE) were retrieved from the Protein Data Bank and were used for the docking studies by means of Surflex-Dock module of SYBYL-X 1.1. The protein was prepared using the Biopolymer application accompanying SYBYL according to SYBYL-X 1.1 manual: The bound ligand was extracted from the complexes, water molecules were removed, hydrogen atoms were automatically added, and charges and atom types were assigned according to AMBER99. After the protomol was generated, which referred to a computational representation of the intended binding site to which putative ligands are aligned, the optimized compounds **Ij** and GW678248 were docked into NNIBP, with the relevant parameters set as defaults. The original ligand of the co-ordinates (3DLE) was used as reference molecule to calculate the RMSD values. The docking scores related to binding affinities were calculated based on hydrophobic, polar, and repulsive interactions as well as entropic effects and solvation. Top-scoring poses of compounds were shown by the software of PYMOL version 0.99 (http://www.pymol.org/). Only the key residues for interactions with the inhibitors were labeled and shown in sticks. The potential hydrogen bonds were presented by dashed lines in red.

Results and Discussion

Chemistry

Newly designed 2-(pyridin-3-yloxy)acetamide derivatives were expeditiously synthesized *via* a very short and efficient route. As shown in Scheme 1, commercially available 2-bromopyridin-3-ol (**S**) was chosen as the starting material, which first reacted with 1-naphthylboric acid or the *p*-substituted phenylboronic acids to afford the key intermediates **I–V**, using K_2CO_3 (in preparing **I**) or K_3PO_4 (in preparing **II–V**) as a base by Suzuki reaction (11). Finally, alkylation at the *OH* group of intermediates **I–V** yielded 23 title compounds **Ia-o, IIa, IIb, IIIa, IIIb, IVa, IVb, Va,** and **Vb** (12). These new compounds were featured by physicochemical and spectral means, and both analytical and spectral data of these target compounds were totally consistent with their molecular structures.

Anti-HIV activity in MT-4 cells

All the target compounds were screened for their *in vitro* anti-HIV activity and cytotoxicity in human T-lymphocyte (MT-4) cell cultures infected with the wt HIV-1 (IIIB) and HIV-2 strain (ROD), respectively. Four compounds were also evaluated for their potency against K103N+Y181C double mutant HIV-1 strain (RES056). The biological

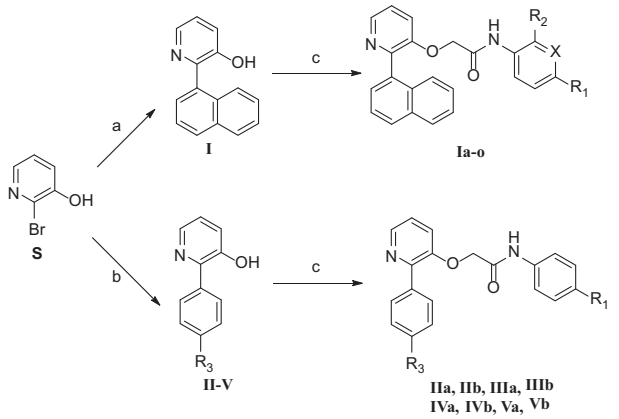

Scheme 1: Reagents and conditions: (a) 1-naphthylboric acid, K_2CO_3, $Pd(PPh_3)_4$, dioxane: water = 5:1, N_2 atmosphere, 90 °C; (b) *p*-substituted phenylboronic acids, K_3PO_4, $Pd(PPh_3)_4$, dioxane: water = 5:1, N_2 atmosphere, 90 °C; (c) $ClCH_2CONHAr$, K_2CO_3, *N,N*-Dimethylformamide (DMF), 50 °C.

results are summarized in Table S1, with nevirapine (NVP), efavirenz (EFV), etravirine (ETR), and zidovudine (AZT) as reference drugs.

As listed in Table S1, these newly synthesized compounds were not as efficient as we expected and were inferior to all the reference drugs NVP (EC_{50} = 0.25 μM), EFV (EC_{50} = 0.0050 μM), ETR (EC_{50} = 0.0041 μM), and AZT (EC_{50} = 0.0058 μM). Among them, three compounds (*viz.* **Ia**, **Ih,** and **Ij**) showed moderate activity against HIV-1 strain (IIIB) with EC_{50} values of 41.5 μM, 10.8 μM, and 8.18 μM, respectively. Of the active compounds, **Ij** was the most potent analogue with an SI value of 2. However, none of the target compounds was effective against the frequently encountered K103N + Y181C double mutant HIV-1 strain and HIV-2 strain.

Further, preliminary SARs were derived from the results described in Table S1. Compared to **II–Va** with the same SO_2NH_2 substituent at 4-position of the right phenyl ring, compound **Ia** kept the moderate activity. On the whole, the potency of subseries **I** was superior to that of subseries **II–V**, indicating a naphthyl substituent was favorable for the anti-HIV-1 activity. What remains to be explained is chloro-pyridine derivative **Ih** (EC_{50} = 10.8 μM) showed increased anti-HIV-1 activity compared to none-substituent derivative **Ii** (EC_{50} >20.2 μM) and other mono-substituent derivatives (**Ia–Ig**) on the right phenyl ring. Moreover, in the bis-substituent subseries (**Ij–Io**), **Ij** with 2-nitro, 4-methyl substituent of the anilide moiety displayed better potency than its counterpart **Ik** (EC_{50} >62.0 μM) and the rest ones. These results were similar with those of arylazolylthioacetanilide NNRTIs.

Regarding the cytotoxicity, it can be observed that **Ih** possessed the lowest cytotoxicity (CC_{50} = 179 μM) and

highest safe profile (SI = 17) in the subseries **I**. The cytotoxicities of subseries **II**–**V** were lower than those of subseries **I** (by comparing **II**–**Va** with **Ia**, or **II**–**Vb** with **Ib**). In addition, in the **I**–**V** subseries, it is noteworthy that compounds bearing a *para*-SO_2NH_2 substituent of the anilide moiety were always found to be less toxic than the *para*-$CONH_2$ substituent derivatives. Besides, in the subseries **I,** the introduction of COMe group in the *para*-position of the anilide moiety gave compounds **Id** and **Il** with pronounced cytotoxicity (CC_{50} = 8.23 μM, 5.51 μM, respectively). As a common sense, the MT-4 cell line is one kind of HTLV-transformed leukemic cells, and thus, we should pay more attention to the molecules with significantly increased cytotoxicities (lower CC_{50} values) to seek drug candidates with potential leukemic/tumoral inhibition serendipitously.

It must be pointed that crystallizations were observed for all the compounds when the anti-HIV screening performed. As physicochemical properties such as water solubility can significantly influence the activities of bioactive molecules (13), the undesired anti-HIV results maybe were related to low solubility.

In brief, although the present molecular modification has not generated very promising leads with improved antiviral potency utilizing this design strategy, the SARs analysis above provided precious clues for further rational design of novel NNRTIs.

Inhibition of HIV-1 RT (wt)

To further confirm the action mechanism of the newly synthesized compounds, four selected derivatives (**Ia**, **Ih**, **Ij,** and **Im**) were tested in recombinant HIV-1 RT inhibitory assays which use poly (A) × oligo $(dT)_{15}$ as template/primer (RT kit; Roche). As shown in Table S2, compound **Ij** still exhibited the most potent inhibitory activity against HIV-1 RT with an IC_{50} value of 38.3 μM among the four compounds, while was much inferior to that of NVP (IC_{50} = 2.32 μM) and ETR (IC_{50} = 0.03 μM). Even though there were some differences between the cell screening test and RT inhibitory assay, the results indicated that the newly designed compounds could act as typical HIV-1 NNRTIs, but their abilities of binding with RT were insufficient which needed to be improved by further modifications.

Molecular modeling analysis

Molecular modeling was carried out to further investigate the possible binding mode of the target compounds in NNIBP of RT. The representative compound **Ij** and the lead compound GW678248 were docked into the NNIBP (PDB code: 3DLE) by Surflex-Dock module of SYBYL-X 1.1 software, and the docking results were shown by PYMOL 0.99. Default parameters were used as described in the SYBYL-X 1.1 manual unless otherwise specified.

As shown in Figure S4, the detailed binding pattern analysis can be described as follows: (i) The pyridine ring of compound **Ij** fits into a hydrophobic subpocket, which is surrounded by the aromatic side chains of Tyr181, Tyr188, Phe227, and Trp229. Particularly, it is parallel to the side-chain phenyl group of Tyr188, generating face-to-face π–π interactions. And the naphthyl group, which located in the middle of NNIBP, is also parallel to the side-chain phenyl group of Tyr181. Those features are distinct from those for GW678248: The 3-chloro-5-cyanobenzene motif is located in the aromatic-rich subpocket, while the center phenyl ring is far away from these aromatic residues. (ii) The anilide moiety of **Ij** is positioned under the residue His235 and is oriented directly toward the RT/solvent interface. In addition, the oxygen of NO_2 forms a hydrogen bond with the backbone *NH* of Lys103, which was very important in the arylazolylthioacetanilide NNRTIs (14–16). (iii) Moreover, it is found that the *NH* of **Ij** can form double hydrogen bonds with the backbone carbonyl oxygen of His235 and side-chain hydroxyl oxygen of Tyr318. By contrast, one hydrogen bond is formed between the SO_2NH_2 substituent of GW678248 and the backbone carbonyl of Lys104. The triple hydrogen bonds between **Ij** and NNIBP would favor the binding affinity and may be responsible for its moderate anti-HIV-1 potency.

In silico calculation of physicochemical properties

Furthermore, some physicochemical properties of the active HIV-1 inhibitors **Ia**, **Ih**, **Ij** and the lead compound GW678248 (as control) were calculated using the free online MOLINSPIRATION software (http://www.molinspiration.com/). The predicted results were presented in Table S3. The physicochemical studies suggested that the three compounds and GW678248 conformed the Lipinski's rule of five well, but the former ones could not show the excellent antiviral potency as GW678248. There would be other factors, which might be responsible for their reduced inhibitory activities.

Conclusions

Briefly, based on the structures of previously reported lead compounds GW678248 and parazole oxyacetamide derivative **3**, we designed and synthesized a series of novel anti-HIV-1 agents by employing a structure-based molecular hybridization and bioisosterism approach. Antiviral screening results showed that three compounds (**Ia**, **Ih,** and **Ij**) displayed moderate potency against wt HIV-1 strain (III_B) with EC_{50} values ranging from 8.18 to 41.52 μM. Among them, **Ij** was the most active analogue possessing an EC_{50} value of 8.18 μM. Preliminary SAR analysis was discussed in detail. Four compounds were selected to implement an HIV-1 RT inhibitory assay to confirm the binding target. Some predicted physicochemical properties of the three active compounds **Ia**, **Ih,** and **Ij** were studied. Molecular docking studies were also carried out to

investigate the binding modes of **Ij** and GW678248 in the binding pocket of RT, which provided beneficial information for further rational design of NNRTIs.

Acknowledgments

The financial support from the Key Project of NSFC for International Cooperation (No. 81420108027, 30910103908), National Natural Science Foundation of China (NSFC No. 81102320, 81273354), Research Fund for the Doctoral Program of Higher Education of China (No. 20110 131130005), Natural Science Foundation of Shandong Province (ZR2009CM016) and KU Leuven (GOA 10/014) is gratefully acknowledged. We thank K. Erven, K. Uytterspot and C. Heens for technical assistance with the anti-HIV assays.

Conflict of Interest

The authors declare no conflict of interest.

References

1. Zhan P., Chen X., Li D., Fang Z., De Clercq E., Liu X. (2013) HIV-1 NNRTIs: structural diversity, pharmacophore similarity, and implications for drug design. Med Res Rev;33(Suppl 1):E1–E72.
2. Huang B., Liang X., Li C., Chen W., Liu T., Li X., Sun Y., Fu L., Liu H., De Clercq E., Pannecouque C., Zhan P., Liu X. (2015) Fused heterocycles bearing bridgehead nitrogen as potent HIV-1 NNRTIs. Part 4: design, synthesis and biological evaluation of novel imidazo [1,2-a]pyrazines. Eur J Med Chem;93:330–337.
3. Li D., Zhan P., De Clercq E., Liu X. (2012) Strategies for the design of HIV-1 non-nucleoside reverse transcriptase inhibitors: lessons from the development of seven representative paradigms. J Med Chem;55:3595–3613.
4. Monforte A.-M., Ferro S., De Luca L., Lo Surdo G., Morreale F., Pannecouque C., Balzarini J., Chimirri A. (2014) Design and synthesis of N1-aryl-benzimidazoles 2-substituted as novel HIV-1 non-nucleoside reverse transcriptase inhibitors. Bioorg Med Chem;22:1459–1467.
5. Ren J., Chamberlain P.P., Stamp A., Short S.A., Weaver K.L., Romines K.R., Hazen R., Freeman A., Ferris R.G., Andrews C.W., Boone L., Chan J.H., Stammers D.K. (2008) Structural basis for the improved drug resistance profile of new generation benzophenone non-nucleoside HIV-1 reverse transcriptase inhibitors†. J Med Chem;51:5000–5008.
6. Ferris R.G., Hazen R.J., Roberts G.B., St Clair M.H., Chan J.H., Romines K.R., Freeman G.A., Tidwell J.H., Schaller L.T., Cowan J.R., Short S.A., Weaver K.L., Selleseth D.W., Moniri K.R., Boone L.R. (2005) Antiviral activity of GW678248, a novel benzophenone nonnucleoside reverse transcriptase inhibitor. Antimicrob Agents Chemother;49:4046–4051.
7. Gagnon A., Landry S., Coulombe R., Jakalian A., Guse I., Thavonekham B., Bonneau P.R., Yoakim C., Simoneau B. (2009) Investigation on the role of the tetrazole in the binding of thiotetrazolylacetanilides with HIV-1 wild type and K103N/Y181C double mutant reverse transcriptases. Bioorg Med Chem Lett;19:1199–1205.
8. Pannecouque C., Daelemans D., De Clercq E. (2008) Tetrazolium-based colorimetric assay for the detection of HIV replication inhibitors: revisited 20 years later. Nat Protoc;3:427–434.
9. Pauwels R., Balzarini J., Baba M., Snoeck R., Schols D., Herdewijn P., Desmyter J., De Clercq E. (1988) Rapid and automated tetrazolium-based colorimetric assay for the detection of anti-HIV compounds. J Virol Methods;20:309–321.
10. Suzuki K., Craddock B.P., Okamoto N., Kano T., Steigbigel R.T. (1993) Poly A-linked colorimetric microtiter plate assay for HIV reverse transcriptase. J Virol Methods;44:189–198.
11. D'Angelo N.D., Bellon S.F., Booker S.K., Cheng Y., Coxon A., Dominguez C., Fellows I. *et al.* (2008) Design, synthesis, and biological evaluation of potent c-Met inhibitors. J Med Chem;51:5766–5779.
12. Rai D., Chen W., Zhan P., Liu H., Tian Y., Liang X., De Clercq E., Pannecouque C., Balzarini J., Liu X. (2014) Synthesis and anti-HIV activity of 4-(naphthalen-1-yl)-1,2,5-thiadiazol-3-hydroxyl derivatives. Chem Biol Drug Des;84:420–430.
13. Huang B., Li C., Chen W., Liu T., Yu M., Fu L., Sun Y., Liu H., De Clercq E., Pannecouque C., Balzarini J., Zhan P., Liu X. (2015) Fused heterocycles bearing bridgehead nitrogen as potent HIV-1 NNRTIs. Part 3: optimization of [1,2,4]triazolo[1,5-a] pyrimidine core via structure-based and physicochemical property-driven approaches. Eur J Med Chem;92:754–765.
14. Zhan P., Liu X., Li Z., Fang Z., Li Z., Wang D., Pannecouque C., Clercq E.D. (2009) Novel 1,2,3-thiadiazole derivatives as HIV-1 NNRTIs with improved potency: synthesis and preliminary SAR studies. Bioorg Med Chem;17:5920–5927.
15. Zhan P., Chen X., Li X., Li D., Tian Y., Chen W., Pannecouque C., De Clercq E., Liu X. (2011) Arylazolylthioacetanilide. Part 8: design, synthesis and biological evaluation of novel 2-(2-(2,4-dichlorophenyl)-2H-1,2,4-triazol-3-ylthio)-N-arylacetamides as potent HIV-1 inhibitors. Eur J Med Chem;46:5039–5045.
16. Zhan P., Li X., Li Z., Chen X., Tian Y., Chen W., Liu X., Pannecouque C., De Clercq E. (2012) Structure-based bioisosterism design, synthesis and biological evaluation of novel 1,2,4-triazin-6-ylthioacetamides as potent HIV-1 NNRTIs. Bioorg Med Chem Lett;22:7155–7162.

Supporting Information

Additional Supporting Information may be found in the online version of this article:

Figure S1. Structures of FDA-approved NNRTIs.

Figure S2. Structures of lead compounds **GW678248** (**1**), **2** and **3**.

Figure S3. Design of 2-(pyridin-3-yloxy)acetamide derivatives.

Figure S4. The predicted binding modes of compound **Ij** (yellow) and lead compound **GW678248** (green) in NNIBP (PDB code: 3DLE). Hydrogen bonds are indicated with dashed lines in red.

Table S1. *In vitro* anti-HIV-1 activity and cytotoxicity of target compounds (**Ia-o**, **IIa**, **IIb, IIIa, IIIb, IVa, IVb, Va, Vb**).

Table S2. Inhibitory activity of compounds **Ia**, **Ih**, **Ij**, **Im**, **NVP** and **ETR** against HIV-1 RT.

Table S3. Prediction of physicochemical properties of **Ia**, **Ih**, **Ij** and **GW678248**.

Appendix S1. Physical properties and spectrum data of target compounds.